EXPERIMENTAL AND THEORETICAL STUDY OF AIRFLOW IN GRAIN BULKS UNDER ANISOTROPIC CONDITIONS

Oleg Khatchatourian, olegkha@unijui.edu.br
Nelson Toniazzo, toniazzo@unijui.edu.br
Fernando Tosini, fernandotosini @hotmail.com
Department of Physics, Statistics and Mathematics, Regional University of the Northwest, Rio Grande do Sul, R. São Francisco, 501, 98700-000, IJUÍ RS, Brazil

Yury Gortyshov, rector@kai.ru
Department of Theory of Heat Transfer, Tupolev Kazan State Technical University, 10, K. Marx St., Kazan, 420111, Russia

Abstract. *A mathematical model, algorithm, and software were developed to calculate the static pressure, streamlines, and airflow velocity distribution in grain bulks for two- and three-dimensions under anisotropic conditions. The empirical relationships between permeability factors in horizontal and vertical directions (anisotropy factors) were analysed for soybean, wheat, maize, oats, rice, peas, flax seed and lentils mass. It was showed that anisotropy factor depends on the grain form and increases significantly with a deviation of this form from spherical. Anisotropy factor is rising with increase in air velocity, and the velocity influence rate varies from very weak for seeds with the form close to spherical (peas, soybean), up to essential, for grains with a greater deviation of the form from spherical (lentils, rice). In this work the relationship between the maximal area of grain contour projection on a horizontal plane (midsection for vertical flow) and the most probable value of the area of grain contour projection on a vertical plane (midsection for horizontal flow) was used as the principal parameter to specify the anisotropy factor of an anisotropy granular medium. As simulations show, there is difference between airflows through isotropic and anisotropic medium. This difference depends on grain type (value of anisotropy factor), area cross-section variation of storage bin (expansion ratio) and air inlet location. It was carried out numerical simulations of real and hypothetical aerated grain stores to detect the anisotropy influence on operational risk areas.*

***Keywords**: Aeration, Anisotropy medium, 3-D airflow simulation, Aerated grain storage bins, Finite-element method*

1. INTRODUCTION

Aeration (forced convection, ventilation) is widely used in grain stores to maintain and preserve the grain quality. Airflow distribution in grain bulk depends on various factors, including the filling method and grain bulk porosity, the depth of the grain, the grain morphology and configuration and size of the interstitial space in the mass, the air velocity, the form and size of any extraneous impurity in the mass, etc.

The influence of some of these parameters on airflow pattern in grain bulk has been studied by Shedd (1953), Brooker (1961 and 1969), Brooker *et al*. (1982), Bunn and Hukill (1963), Pierce and Thompson (1975), Haque *et al*. (1981), Jayas *et al.* (1987), Maier *et al*. (1992), Weber (1995), Navarro and Noyes (2001), Khatchatourian and Savicki (2004), Crozza and Pagano (2006), Khatchatourian and Oliveira (2006), and Oliveira *et. al.* (2007). Gayathri and Jayas (2007) have presented a review of the reported mathematical models of airflow through grain mass.

In large storage bins non-homogeneity of grain mass significantly affects flow field. Khatchatourian and Binelo (2008) have researched the compaction of the grain and the airflow pattern under non-homogeneous conditions.

As works Hood and Thorpe (1992), Neethhirajan *et al*. (2006 and 2008) showed, there is a strong anisotropy of medium resistance to airflow through grain mass. For airflow in a silo where the area of cross-section as well as airflow direction practically does not vary, this effect can be neglected. However for the large grain storage bins with variable area the effect of anisotropy can be essential. Besides, the aeration of large grain stores is frequently carried out separately in different segments, thus, a vertical velocity component is not predominant in these conditions.

The principal objectives of the present work were:

(a) to create a mathematical model, algorithm, and software, to calculate the static pressure, streamlines, and airflow velocity distribution in two- and three-dimensions under anisotropic conditions;

(b) to study the relationship between the air velocity and the pressure gradient as a function of the pipe diameter, bed depth, filling method and airflow direction for wheat, oats, maize, rice and soybean mass; and

(c) to carry out numerical simulations of real and hypothetical grain stores with aeration to detect the anisotropy influence on operational risk areas.

2. MATHEMATICAL MODEL

The incompressible viscous isothermal flow is governed by the system of equations of continuity [Eq. (1)] and of Navier-Stokes [Eq. (2)]:

$$\operatorname{div} \boldsymbol{V} = 0 \tag{1}$$

$$\rho \frac{\mathrm{D}\boldsymbol{V}}{\mathrm{D}t} = -\mathrm{grad}P + \mu \nabla^2 \boldsymbol{V} \tag{2}$$

where: $\boldsymbol{V}$ is the velocity vector in m s^{-1}; ρ is the density in kg m^{-3}; t is the time in s; P is the pressure in Pa; μ is the dynamic viscosity in Pa s.

Usually for problems of airflow through grain bulks, the Eq. (2) is replaced by empirical dependence $\boldsymbol{V} = \boldsymbol{f}(\mathrm{grad}P)$, that represents nonlinear motion equation. In most of these equations the gradient of pressure is expressed as function of velocity by second-order parabola without a free term (Scheidegger 1960, Bear 1988).

The basic results of works for pressure-drop modelling in stored grain masses are complied in ASAE (2000) and Navarro and Noyes (2001). In both these works it was used two-parameter model of Hukill and Ives (1955).

As work Khatchatourian and Binelo (2008) showed, in large grain storage conditions it is more preferable to use three-parameter models, which permit to describe both the function $\boldsymbol{V} = \boldsymbol{f}(\mathrm{grad}P)$ and its derivative. Their mathematical model, used in present study for simulation of the airflow for 2D and 3D cases, consists of a system:

$$\operatorname{div} \boldsymbol{V} = 0 \tag{3}$$

$$\boldsymbol{V} = -\frac{\mathrm{grad}P}{|\mathrm{grad}P|} \exp\left(\left\{\left[\ln\left(1+U^2\right) - 2U\arctan(U)\right]/\pi + 3U\right\}/4a + c\right) \tag{4}$$

where $U = a \ln|\mathrm{grad}P| + b$ é an intermediate argument; $a>0$, b e c are constants.

Eq. (4), which has replaced the Navier-Stokes equation, for 2D or 3D case can be written in the form:

$$\boldsymbol{V} = -\boldsymbol{K} \cdot \mathrm{grad}P \tag{5}$$

where $\boldsymbol{K}$ is the second-rank hydraulic conductivity tensor for anisotropic medium. For isotropic non-homogeneous medium $K=K(x,y,z)$ is scalar.

If x, y, z are principal directions (which are collinear to eigenvectors of matrix $\boldsymbol{K}$), the tensor $\boldsymbol{K}$ has diagonal form. In this case the velocity components u, v and w for the three-dimensional case can be expressed in the form:

$$u = -K_x \frac{\partial P}{\partial x}; v = -K_y \frac{\partial P}{\partial y}; w = -K_z \frac{\partial P}{\partial z} \tag{6}$$

Substituting Eq. (5) in Eq. (3), the nonlinear partial differential equation is obtained:

$$\frac{\partial}{\partial x}\left(-K_x \frac{\partial P}{\partial x}\right) + \frac{\partial}{\partial y}\left(-K_y \frac{\partial P}{\partial y}\right) + \frac{\partial}{\partial z}\left(-K_z \frac{\partial P}{\partial z}\right) = 0 \tag{7}$$

The boundary conditions for the problem considered have the form:

$P=P_e$ (Dirichlet condition for air entrance and exit) (8)

$\boldsymbol{n} \cdot K \cdot \mathrm{grad}P = 0$ (Neumann condition on the walls and floor of the silo) (9)

where P_e is air entrance or exit pressure in Pa; and $\boldsymbol{n}$ is unit vector normal to the wall or floor surface.

Eq. (7) along with the boundary conditions Eq. (8) and Eq. (9) describes the steady-state pressure and velocity distributions in a cross-section of aerated grain storage under non-uniform and anisotropic conditions. It is possible to admit, that $K_x = K_z \neq K_y$ and that coefficient of permeability K_y is defined by the expression obtained of Eq. (4):

$$K_y = \exp\left(\left\{\left[\ln\left(1+U^2\right) - 2U\arctan(U)\right]/\pi + 3U\right\}/4a + c\right)/|\mathrm{grad}P| \tag{10}$$

The dependences for K_x and K_z can be obtained experimentally for each kind of grain.

The streamlines for 3D case can be calculated using the obtained velocity distribution. For 2D case it is easier to solve the partial differential equation of Lagrange stream functions Ψ for non-homogeneous anisotropic medium:

$$\frac{\partial}{\partial x}\left(\frac{1}{K_y}\frac{\partial \Psi}{\partial x}\right)+\frac{\partial}{\partial y}\left(\frac{1}{K_x}\frac{\partial \Psi}{\partial y}\right)=0 \quad (11)$$

3. EXPERIMENTAL APPARATUS

To simulate the aerated grain storage characteristics, the equipment, showed in Fig.1, was used. The experimental equipment consists of a centrifugal fan, an orifice-plate and a system of four small 'silos' composed of a polyvinyl chloride tubes (inside diameters from 0.05 m to 0.2 m and height of 1 m.

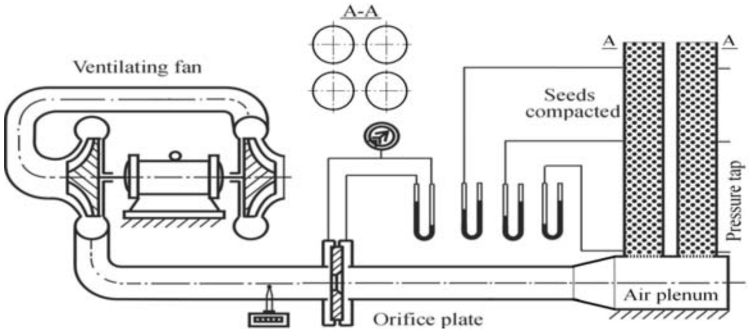

Fig. 1 - Sketch of the experimental equipment

The study was done for wheat, oats, maize, rice and soybean. The grain characteristics were obtained in the Laboratory of Seeds Analysis, Department of Agrarian Studies, Regional University of the Northwest, Rio Grande do Sul – UNIJUI, Brazil. Grains, used in the tests, had a moisture content of 11-13%. Impurities were less than 2%.

3.1. Experimental design

Four types of experiments were accomplished for five kinds of seed to determine:
1) The influence of filling method and of exit grate presence on airflow resistance. As test column it was used a cube with side = 0.4 m.
2) The influence of pipe diameter and depth of grain mass on airflow resistance. The pipe diameters *D* were of 0.05 m, 0.075 m, 0.1 m, 0.15 m and 0.2 m. The depths of grain mass *H* were: 0.2 m, 0.4 m, 0.6 m, 0.8 m, 1 m and 3 m.
3) The influence of airflow direction (vertical or horizontal) on airflow resistance. It was used a cube with side = 0.4 m.
4) The relationship between airflow and pressure gradient for five kinds of seed (wheat, oats, maize, rice and soybean).

3.2. Filling method and influence of exit grate presence

The method to fill the grain column essentially influences on resistance to airflow of grain mass (Kumar & Muir 1986, Navarro & Noyes 2001). Two methods which used a filling funnel were analyzed in present work. In the first method the exit funnel section was located near to a grain surface and been moved in a cross-section direction, spreading smoothly the seeds layer by layer and uniformly increasing the depth. In the second method, which was selected for all of posterior experiments, the exit section of motionless funnel was fixed in the top of column.

3.3. Selection of diameter and depth bed of experimental camera

There are many experimental works for study of airflow in grain bulks. The basic results of these works concentrated in ASAE (2000), ASAE Standards 2000 D272.3 MAR96 and in Navarro and Noyes (2001) were obtained under different conditions using experimental cameras of different dimensions.

In present work in particular, it was analyzed the influence of pipe diameter and depth bed on resistance to airflow of grain mass.

To maintain the measurement accuracy of pressures two orifice plates were used (one for low and other for usual airflow). To increase the limits of air velocity variation inside of experimental camera the 'small silos' of various diameters 0.05 m, 0.075 m, 0.1 m, 0.15 m and 0.2 m were used. To expand still more the inferior limit and at the same time to increase the quantity of experimental data it was built a plenum with one entrance and four exits for tubes of same diameters (*D*=0.05 m, 0.075 m, 0.1 m, 0.15 m and 0.2 m). The depth bed *H* of each 'small silo' was chosen of 0.2 m, 0.4 m, 0.6 m, 0.8 m and 1.0 m.

Experimental data show that the increase of pipe diameter from 0.05 m to 0.1 m reduces the resistance of grain layer of the same depth. The posterior increase (from 0.1 m to 0.2 m) doesn't influence on resistance.

The analysis of dependence between dimensionless depth H/D and a pressure gradient shows, that for $H/D > 3$ the value of a pressure gradient can be considered constant for all studied grain kinds. The decrease of H/D from 3 up to 1 reduces pressure gradient for soybean and wheat bulks and increases for rice and oats bulks. For maize bulk a value of pressure gradient can be considered constant for all studied interval of dimensionless depth variation (from 1 to 10).

Thus, the obtained results allowed to find the minimal diameter of experimental camera (≈ 0.1 m) and the minimal depth bed (≈ 0.4 m) for analysis of resistance to airflow of grain mass, for which the experimental results don't depend on dimensions of the equipment. Therefore to obtain the empiric dependences the cameras of diameters of 0.1 m, 0.15 m and 0.2 m were used. The used depth beds were 0.6 m, 0.8 m and 1.0 m.

4. VALIDATION OF THE MATHEMATICAL MODEL FOR NON-HOMOGENEOUS ANISOTROPIC CONDITIONS IN A GRAIN BULK

The elements of the hydraulic conductivity tensor $\boldsymbol{K}$ used in Eqs. (7) and (11) have been determined of the relationship between velocity $\boldsymbol{V}$ and pressure gradient grad$P$ along vertical and horizontal directions obtained experimentally. To estimate the anisotropy in this work it was used the anisotropy factor defined as the ratio of the effective (macroscopic) hydraulic conductivities along vertical and horizontal directions.

4.1. Relationship between air velocity and air pressure drop along vertical direction

Fig. 6 presents the relationship between air velocity V in m s^{-1} and air pressure drop obtained experimentally for vertical direction of airflow. Table 1 contents the values of coefficients a, b and c for soybean, maize, rice and wheat obtained by LS method for dependence (4). These data permit to calculate K_y in Eq. (10).

Table 1. The empirical coefficients a, b and c with 95% confidence bounds for different seeds, sum squared error (SSE), coefficient of determination (R^2) and root mean squared error (standard error) for Eq. (4) .

	a	b	c	SSE	R^2	RSME
Soybean	0.82±0.12	-3.57±0.66	-2.77±0.12	0.5013	0.9954	0.0480
Maize	0.61±0.07	-2.92±0.39	-2.75±0.08	0.1304	0.9982	0.0289
Rice	0.51±0.13	-3.08±0.82	-2.23±0.13	0.3526	0.9934	0.0525
Wheat	0.86±0.15	-5.49±0.98	-2.18±0.06	0.1296	0.9972	0.0348

4.3. Relationship between permeability coefficients along horizontal and vertical directions

If x, y, z are principal directions the anisotropy factor can be estimated by ratio $\dfrac{K_x}{K_y} = \dfrac{\partial P}{\partial y} \Big/ \dfrac{\partial P}{\partial x}$, which in this work was determined experimentally. Fig. 7 presents the anisotropy factor variation with velocity for various grain types.

It is possible to see, that the grains having a greater eccentricity, form a medium with greater anisotropy factor. For example, this factor is almost equal to 1 for the peas which possess a nearly spherical form. On the contrary, anisotropy factor values for lentils and oats are much greater.

As Fig. 8 shows, dependence between $\ln(K_x/K_y)$ and $\ln(V)$ can be considered as linear ($R^2 > 0.943$), *i.e.* can be presented in the form:

$$\ln\left(K_x / K_y\right) = s \ln V + d \,, \tag{12}$$

where s is slope and d is constant term.

Anisotropy factor defined by ratio K_x/K_y depends on Reynolds number (by means of air velocity and grain morphology) and represents an airflow dynamics characteristic. Thus, it can be named 'aerodynamics' or 'hydrodynamics' anisotropy factor. Even for different grain bulks its anisotropy factors can be equal at different corresponding velocities.

To generalize all results for static granular medium generated by any kind of seeds it is necessary to define the characteristic parameter (or parameters combination) of this medium which determines an airflow difference in vertical and horizontal directions, *i.e.* to relate s and d in Eq. (12) with geometric characteristics of grains formed the porous medium.

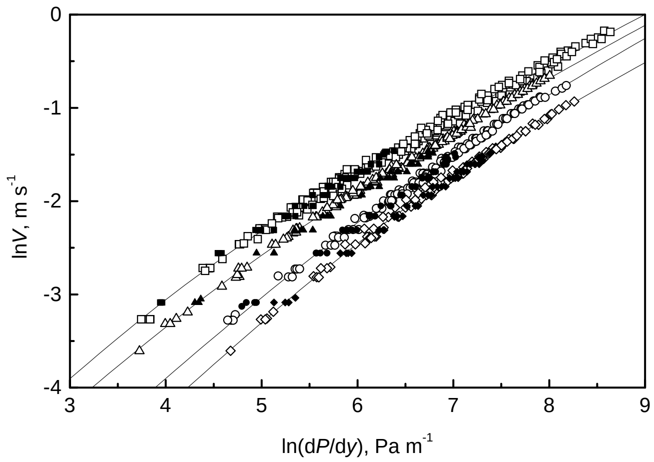

Fig. 6 - Relationship between air velocity and pressure gradient; ■, □, soybean; ▲, △, maize; ●, ○, rice; ♦, ◇, wheat; solid points: cubical box of 0.4 m side; open: tubes of 0.1 m, 0.15m, and 0.2 m diameter; –, predicted by Eq. (4).

At filling, the grains lay down so that the potential energy of system would be the least (the barycentre of each grain tends to occupy the lowest position). It is possible to guess, that value of anisotropy factor for the considered medium is related to the ratio of midsections of grain in vertical and horizontal directions. Let A_{min}, A_{medium}, and A_{max} be the areas of projections of grain contours on its orthogonal sections respective to principal inertia moments (Fig. 9). In this work it is admitted, that both greatest and medium axes of inertia are located in a horizontal plane and midsection of every grain for vertical direction of airflow is constant (A_{max}). The greatest axis of grain can occupy the any direction in this plane and midsection of grain for horizontal airflow varies between A_{medium} and A_{min}. In Fig. 9 this corresponds to a variation of an angle φ between 0 and π/2.

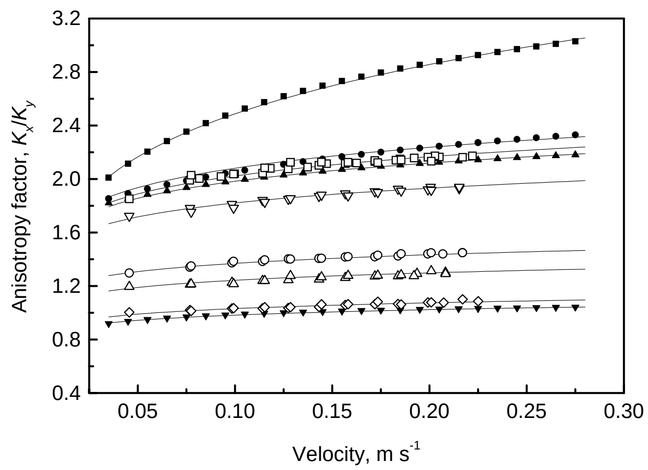

Fig. 7 – Observed and predicted relationships between horizontal and vertical permeability for various seed kind; ■, lentils; ●, flax seed; ▲, white oats; □, rice; ∇, black oats; ○, maize; △, wheat; ◇, soybean; ▼, peas; closed points: Alagusundaram *et. al.* (1992); open points: Authors; –, predicted (Authors).

To generalize the experimental data for anisotropy factor variation the different methods for determination of grain midsection were compared. In particular, it was used the area of grain contour projection: a) in direction of the greatest axis (A_{min}), b) in direction of the intermediate axis (A_{medium}), c) their arithmetic average ($(A_{\mathrm{min}}+A_{\mathrm{medium}})/2$), and, d) their geometrical mean $\sqrt{A_{\mathrm{min}} \cdot A_{\mathrm{medium}}}$. But the best generalization has been obtained at use of most probable estimate area A_{mpe}:

$$A_{\mathrm{mpe}} = \frac{\int_0^{\frac{\pi}{2}} \left(A_{\mathrm{min}} + \left(A_{\mathrm{medium}} - A_{\mathrm{min}}\right)\cos\varphi\right) d\varphi}{\pi/2} = A_{\mathrm{min}} + \frac{2}{\pi}\left(A_{\mathrm{medium}} - A_{\mathrm{min}}\right), \tag{13}$$

where $\varphi \in [0,\pi/2]$ is an angle of deflection of the greatest axis of grain from a plane orthogonal to a horizontal airflow (Fig. 9).

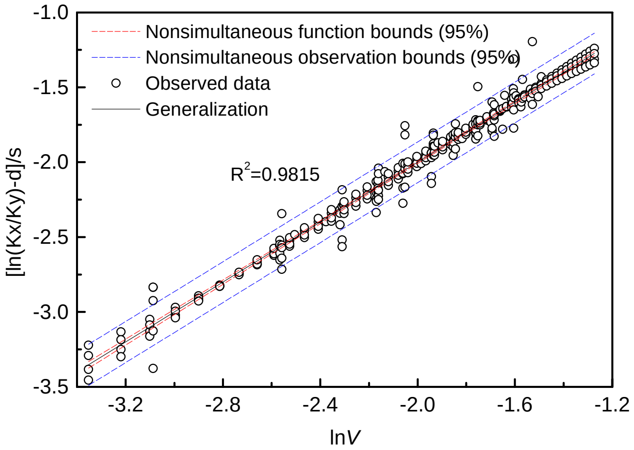

Fig. 8 - Anisotropy factor generalization for various seed kind.

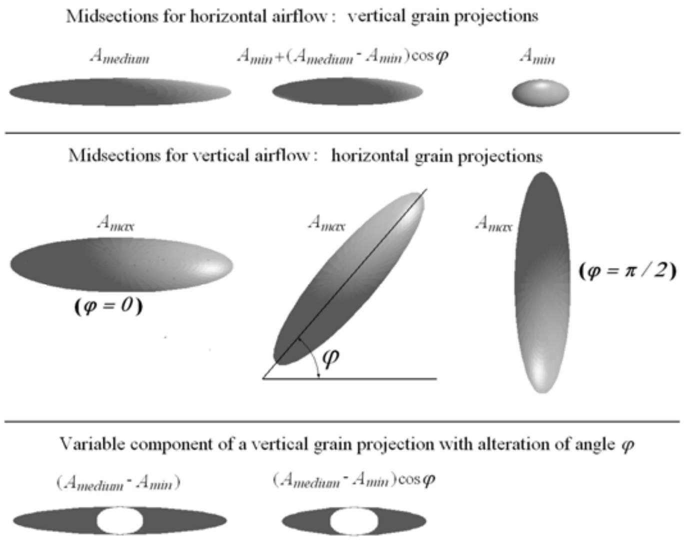

Fig. 9 - The used scheme of calculation of a midsection of grains

Digital image processing was used to obtain the morphological seed characteristics. The image processing was constituted by the following stages: 1) image acquisition: the grain samples were photographed by digital camera DSC-7X, Sony, with resolution of 8 megapixels; 2) pre-processing: an anti-aliasing filter was applied to convert the true-color image to the grayscale intensity image; 3) segmentation: it was made the seeds edges detection (method of Prewitt), edge dilation and removal of needless segments; 4) representation: each seed was represented in the form of a binary matrix 130×130.

Fig. 10 shows the relations between $A_{\max}$ and $(A_{\min}+A_{\mathrm{medium}})/2$, $\sqrt{A_{\min} \cdot A_{\mathrm{medium}}}$ and A_{mpe} for airflow through the rice mass.

The fitted curves for variation of slope s and constant term d of Eq. (12) with variation of ratio $A_{\max}/A_{\mathrm{mpe}}$ obtained by the least square (LS) method were presented in exponential and linear form:

$$s = a_1 \mathrm{e}^{b_1 x} + c_1 , \tag{14}$$

$$d = a_2 x + b_2 , \tag{15}$$

where $x = A_{\max} / A_{\text{mpe}}$; a_1, b_1, c_1, a_2, and b_2 are coefficients, presented in Table 2.

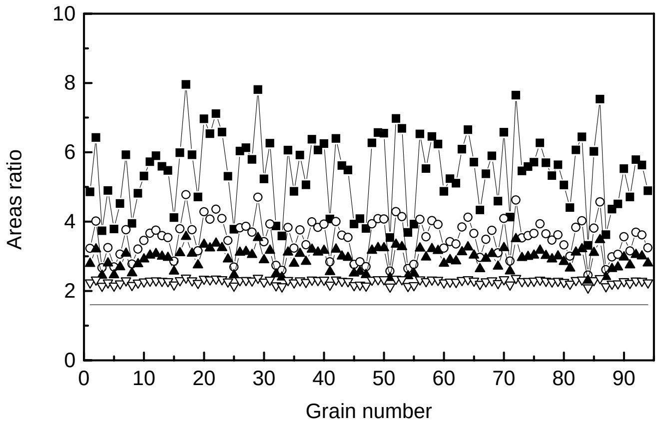

Fig. 10 - Relations between midsection in direction vertical ($A_{\max}$) and examined areas in horizontal plane for rice; ■, $A_{\max}/A_{\min}$;–, $A_{\max}/A_{\text{medium}}$; ○, $A_{\max}/(A_{\text{medium}}+A_{\min})/2$; ▲, $A_{\max}/\sqrt{A_{\min} \cdot A_{\text{medium}}}$; ∇, $A_{\max}/(A_{\min}+2(A_{\text{medium}}-A_{\min})/\pi)$.

Applying these dependences and Eq. (12) for various grain kinds the predicted curves were simulated (continuous lines in Fig. 7).

Table 2. The empirical coefficients a_1, b_1, c_1, a_2, b_2, sum squared error (SSE), coefficient of determination (R^2) and root mean squared error (standard error) for Eqs. (14) and (15).

	a_1	b_1	c_1	a_2	b_2	SSE	R^2	RSME
s, Eq. (14)	0.00083	1.777	0.0528	-	-	0.0002	0.985	0.006
d, Eq. (15)	-	-	-	0.674	-0.591	0.0036	0.999	0.011

Obtained dependences permit to calculate the relationship between velocity and pressure gradient in horizontal direction. In this case there is not a necessity to determinate of constants a, b and c for airflow resistance along horizontal direction. Really, if the grain form is known, it is possible to calculate the ratio $A_{\max} / A_{\text{mpe}}$ and, consequently, s and d for Eq. (12), which determinates the variation of the anisotropy factor with velocity alteration. Applying Eq. (11) with coefficients a, b and c (Table 1) to calculate K_y, it is easy determinate K_x using Eq. (12).

5. SOFTWARE DESCRIPTION AND DEVELOPMENT

The nonlinear partial differential equation for static pressure Eq. (7) was solved by the finite element method (Segerlind, 1976). To calculate the matrix of permeability coefficients in each point of the integration domain it was used an iterative process with using the pressure distribution from the previous iteration step.

The software was developed in ANSI C++ and Dev-Pascal and consisted of tools for geometry construction and mesh generation, generation of system matrix by the finite element method and solver of obtained system of linear algebraic equations and tool for results three-dimensional presentation and analysis. It was used free-of-charge software when possible. To generate mesh it was used Tetgen, available under GPL license. The dynamic adaptive refinement of the mesh (Liu and Joe, 1996), based on a tetrahedron size selection in inverse proportion to the tetrahedron pressure gradient was developed to improve a quality of mesh.

To resolve the problem the software executes four iterative processes: 1) it calculates the hydraulic conductivity tensor for anisotropic medium in each point of the integration domain; 2) it resolves the system of linear algebraic equations by the successive over-relaxation (SOR) method (Hageman and Young, 1981); 3) it searches the system design point, located in the performance curve of the aerator fan; and 4) it adaptively refines the mesh.

For the used scheme of a finite-element method the pressure gradient and consequently the velocity vector are constant inside the simplex element (tetrahedron). To obtain a continuous vector field it was used theory of consistent conjugate approximation (Oden and Reddy, 1973). The full airflow trajectory length (from inlet up to outlet) and the local criterion to estimate the ventilation system performance were calculated for each vertex.

An output file is generated in VTK (Visualization toolkit, http://www.vtk.org/) format. To visualise the results Paraview software (http://www.paraview.org/), available free of charge was used.

6. NUMERICAL SIMULATIONS

To estimate the efficiency of an aeration system in this work it was used the local specific airflow rate introduced in Khatchatourian and Binelo (2008):

$$q_L(X) = \frac{V(X)}{\rho(X)L_X} \tag{16}$$

where $q_L(X)$ is local specific airflow rate in point $X(x,y,z)$ in m^3s^{-1} kg^{-1}; $V(X)$ is air velocity in point X in ms^{-1}; $\rho(X)$ is product density in point X in kg $m^{-3}s^{-1}$; L_X is full length in m of a trajectory on which the point X is located.

6.1. Numerical simulation results

The influence of anisotropy factor on the airflow through grain bulk and on the aeration system efficiency was analyzed for storage bins with three air entrances (Fig. 14). The aeration was carried out: a) simultaneously through all entrances; b) separately through one of three entrances. It was used the global airflow rate of Q=9 m^3 h^{-1} t^{-1} (2.5 $\cdot$ $10^{-6}m^3$ s^{-1} kg^{-1}), which is the most commonly recommended value for aerated grain storage.

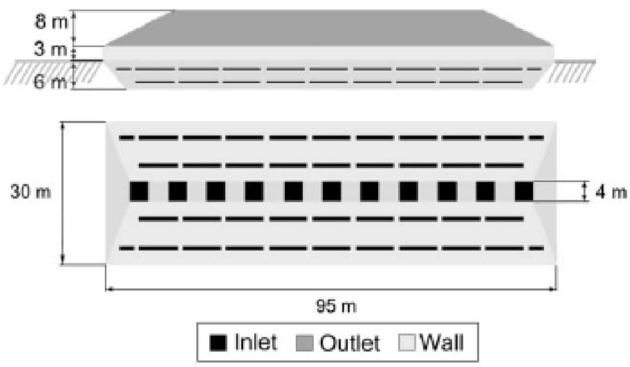

Fig. 14 - Outline sketch of simulated store bin.

Fig. 15 presents the comparison of airflow in central cross-section of storage bins with different aeration systems for anisotropic (A_{max}/A_{mpe}=1.6) and isotropic medium. Four air inlet systems were studied: (a) upper lateral, lower lateral and central inlets; (b) upper lateral inlet; (c) lower lateral inlet; and (d) central inlet.

As simulations show, there is difference between airflows through isotropic (grey lines) and anisotropic (black lines) medium for all considered cases and this difference increases for grain bulks with higher ratio A_{max}/A_{mpe}. Due to larger easiness to move in the horizontal direction in anisotropic medium the air movement increases in this direction. Therefore for airflow through upper lateral inlet (b) and central inlet (d) this difference is more than for airflow through lower lateral inlet (c) or for case of aeration simultaneously through all inlets (a).

To estimate the anisotropy effect on the risk domains in the grain storage bin, the distribution of local specific airflow rates was studied for separated operation of the upper lateral (one time period), lower lateral (two time periods) and central inlets (three time periods).

In Fig. 16 the black lines represent contour curves generated by points with constant values of local airflow specific rates calculated for anisotropic medium. For isotropic medium these curves are represented by white lines.

The values of local specific airflow rate q_L for anisotropic case are more uniform for deep layers. The zone of limited aeration (q_L <3), located in top part of storage bin, increases for anisotropy case, because the part of the air that moved along horizontal direction is more for anisotropic medium than for isotropic medium.

Thus the simulations show, there is difference between airflows through isotropic and anisotropic medium. This difference depends on grain type (value of anisotropy factor), area cross-section variation of storage bin (expansion ratio) and air inlet location. If expansion ratio=1 (for silo case), there is no difference in airflow for isotropic and anisotropic cases.

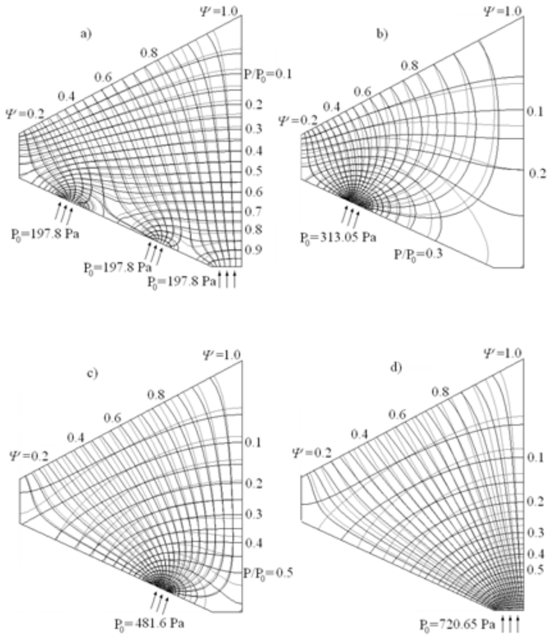

Fig. 15 - Anisotropy influence on airflow in storage bins with different aeration systems; anisotropic medium A_{max}/A_{mpe}=1.6 (maize): black lines; isotropic medium: grey lines.

7. CONCLUSIONS

The ratio of permeability factors in horizontal and vertical directions depends on the grain form and increases significantly with a deviation of this form from spherical. This ratio is rising with increase in air velocity, and the velocity influence rate varies from very weak for seeds with the form close to spherical (peas, soybean), up to essential, for grains with a greater deviation of the form from spherical (lentils, rice). It was showed that the relationship between the maximal area of a grain contour projection on a horizontal plane (midsection for vertical flow) and the most probable value of the area of a grain contour projection on a vertical plane (midsection for horizontal flow) can be used as the principal parameter to specify the anisotropy factor of an anisotropy medium.

As simulations show, there is difference between airflows through isotropic and anisotropic medium. This difference depends on grain type (value of anisotropy factor), area cross-section variation of storage bin (expansion ratio) and air inlet location.

The values of local specific airflow rate q_L for anisotropic case are more uniform for deep layers of aerated storage bin. The zone of limited aeration (q_L <3), located in top part of storage bin, increases for anisotropy case, because the part of the air that moved along horizontal direction is more for anisotropic medium than for isotropic medium.

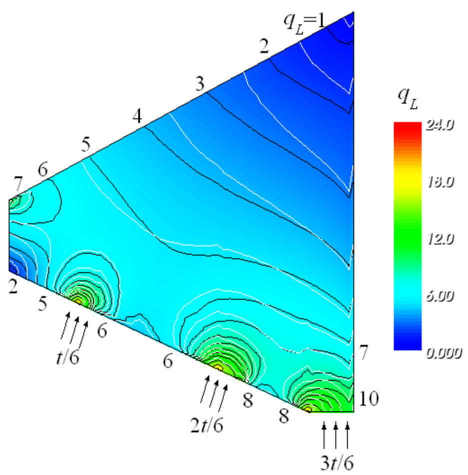

Fig. 16 - Distribution of resultant local specific airflow rates for isotropic (white lines) and anisotropic (black lines) grain bulks with separated functioning inlets, Q=9m^3 h^{-1} t^{-1} (2.5×10^{-6}m^3 s^{-1} kg^{-1}); A_{max}/A_{mpe}=1.6 (maize).

8. REFERENCES

Alagusundaram K; Jayas D S; Chotard F; White N D G (1992). Airflow pressure drop relationships of some specialty seeds. Sciences des Aliments, 12, 101–116

ASAE (2000). Resistance to Airflow of Grains, Seeds, Other Agricultural Products, and Perforated Metal Sheets. American Society of Agricultural Engineers, St. Joseph, MI.

Bear J (1988). Dynamics of Fluids in Porous Media. Dover Publications, New York.

Brooker D B (1961). Pressure patterns in grain drying system established by numerical methods. Transactions of the ASAE, 4, 72–77.

Brooker D B (1969). Computing air pressure and velocity distribution when air flows through a porous medium and nonlinear velocity–pressure relationship exists. Transaction of the ASAE, 12, 118–120.

Brooker D B; Bakker-Arkema F W; Hall C W (1982). Drying Cereal Grains. AVI Publishing Co., Inc., Westport, CT.

Bunn J M; Hukill W V (1963). Pressure pattern prediction for nonlinear air flow through porous medium. Transactions of the ASAE, 6, 32–36.

Crozza D E; Pagano A M (2006). Modelling resistance to airflow through beds of agropyron and corn. Estimation of power ventilation, Latin American Applied Research, 36(1), 1-14

Gayathri P; Jayas D S (2007). Mathematical modeling of airflow distribution in grain bulks – a review. ASAE Annual Meeting 076226, pp. 1–12.

Haque E; Chung D S; Forster G H (1981). Pressure and velocity field in airflow through packed bed of corn with fines non-Darcy flow conditions. Transactions of the ASAE, 5, 1595–1604.

Hood T J A; Thorpe G R (1992). The effects of the anisotropic resistance to airflow on the design of aeration systems for bulk stored grains. Agricultural Engineering Australia, 21, 18-23.

Hukill W V; Ives N C (1955). Radial airflow resistance of grain. Agricultural Engineering, 36, 462–466.

Jayas D.S., Sokhansanj S., Moysey E.B., Barber E.M. (1987). The effect of airflow direction on the resistance of canola (rapeseed) to airflow. Canadian Agricultural Engineering, 29, 189-192.

Khatchatourian O A; Binelo M O (2008). Simulation of three-dimensional airflow in grain storage bins. Biosystems Engineering, 101(2), 225–238.

Khatchatourian O A; de Oliveira F A (2006). Mathematical modelling of airflow and thermal state in large aerated grain storage. Biosystems Engineering, 95(2), 159–169.

Khatchatourian O A; Savicki D L (2004). Mathematical modelling of airflow in an aerated soybean store under non-uniform conditions. Biosystems Engineering, 88(2), 201–211.

Kumar A, Muir W E (1986). Airflow resistance of wheat and barley affected by airflow direction, filling method and dockage. Transactions of the ASAE, 29, 1423-1426

Liu A; Joe B (1996). Quality local refinement of tetrahedral meshes based on 8-subtetrahedron subdivision. Mathematics of Computation, 65(215), 1183–1200.

Maier D E; Moreira R G; Bakker-Arkema FW (1992). Comparison of conventional and chilled aeration of grains under Texas conditions. Applied Engineering in Agriculture, 8(5), 661–667.

Navarro S; Noyes R T (eds) (2001). CRC Press LLC, USA.

Neethirajan S; Jayas D S; White N D G; Zhang H (2008). Investigation of 3D geometry of bulk wheat and pea pores using X-ray computed tomography images. Computers and Electronics in Agriculture, 63(2), 104–111.

Neethirajan S; Karunakaran C; Jayas D S; White N D G (2006). X-ray computed tomography image analysis to explain the airflow resistance differences in grain bulks. Biosystems Engineering, 94(4), 545–555

Oden J T; Reddy J N (1973). Note on an approximate method for computing consistent conjugate stresses in elastic finite elements. International Journal for Numerical Methods in Engineering, 6, 55–61.

Oliveira F A; Khatchatourian O A; Bihain A (2007). Estado térmico de produtos armazenados em silos com sistema de aeração: estudo teórico e experimental. [Thermal state of stored products in storage bins with aeration system: experimental-theoretical study]. Engenharia Agrícola, 27(1), 247-258.

Pierce R O; Thompson T L (1975). Airflow pattern in coaxial-shaped piles of grain. Transactions of the ASAE, 18, 946–949.

Nalladurai K; Alagusundaram K; Gayathri P (2002), Airflow resistance of paddy and its byproducts, Biosystems Engineering, 83(1), 67-75

Scheidegger A E (1960). The Physics of Flow through Porous Media (2nd ed.). University of Toronto Press, Toronto.

Segerlind L J (1976). Applied Finite Element Analysis. J. Wiley and Sons Inc., New York, USA.

Shedd C K (1953). Resistance of grains and seeds to air flow. Agricultural Engineering, 34(9), 616–619.

Weber E (1995). Armazenagem Agrícola [Agricultural storage]. Kepler Weber Industrial, Porto Alegre.

9. RESPONSIBILITY NOTICE

The authors are the only responsible for the printed material included in this paper.